Symmetry Breaking in Cationic Polymethine Dyes, Part 1: Ground State Potential Energy Surfaces and Solvent Effects on Electronic Spectra of Streptocyanines

6 AUTHORS, INCLUDING:

Tzvetelin D. Iordanov

Georgia Southwestern State University

13 PUBLICATIONS **496** CITATIONS

SEE PROFILE

Artem E. Masunov

University of Central Florida

147 PUBLICATIONS **2,534** CITATIONS

SEE PROFILE

Andrew Levenson

2 PUBLICATIONS **17** CITATIONS

SEE PROFILE

Olga V Przhonska

National Academy of Sciences of Ukraine

106 PUBLICATIONS **1,616** CITATIONS

SEE PROFILE

Symmetry Breaking in Cationic Polymethine Dyes, Part 1: Ground State Potential Energy Surfaces and Solvent Effects on Electronic Spectra of Streptocyanines

TZVETELIN D. IORDANOV,[1] JESSE L. DAVIS,[1]
ARTËM E. MASUNOV,[2,3] ANDREW LEVENSON,[2,3]
OLGA V. PRZHONSKA,[4] ALEXEI D. KACHKOVSKI[5]

[1]*Department of Chemistry, Georgia Southwestern State University, 800 Wheatley Street, Americus, GA 31709*

[2]*Department of Chemistry, NanoScience Technology Center, University of Central Florida, 12424 Research Parkway, Ste 400, Orlando, FL 32826*

[3]*Department of Physics, NanoScience Technology Center, University of Central Florida, 12424 Research Parkway, Ste 400, Orlando, FL 32826*

[4]*Institute of Physics, National Academy of Sciences, Prospect Nauki 46, Kiev, 03028, Ukraine*

[5]*Institute of Organic Chemistry, National Academy of Sciences, Murmanskaya 5, Kiev 03094, Ukraine*

ABSTRACT: Charge localization and dynamics in conjugated organic molecules, as well as their spectral signatures are of great importance for photonic and photovoltaic applications. Intramolecular charge delocalization in polymethine dyes occurs through π-conjugated bridges and contributes to the appearance of low-energy excited states that strongly influence their linear and nonlinear optical (NLO) properties. When the chain length in symmetrical cations exceeds the characteristic size of the soliton, the positive charge may localize at one of the terminal groups of the molecule and induce symmetry breaking of both the electron density distribution and molecular geometry.

This charge localization is coupled with molecular vibrations and solvent effects. We investigated the mechanism of symmetry breaking in a series of cationic streptocyanines with different conjugated chain length and qualitatively predicted their electronic absorption spectra. This class of organic molecules is chosen as a model system to develop methodology which can subsequently be used to evaluate more complicated compounds for NLO applications. Our calculations show that the minimum number of vinylene groups in the conjugated chain necessary to break the symmetry of streptocyanines is eight in the gas phase and six in cyclohexane. We constructed the ground state potential energy surface (PES) in two dimensions using symmetry breaking and symmetry adapted coordinates. These were defined as the difference and the sum of the two central carbon–carbon bonds, respectively. This PES was found to have two equivalent minima for systems with symmetry breaking. The energy barrier between these two minima was estimated in the gas phase and in solution, which was taken into account by the polarizable continuum model. Charge localization in each minimum was found to be asymmetric. It is additionally stabilized by the solvent reaction field, which increases the energy barrier. The electronic absorption spectrum in solution is red shifted as compared to the gas phase. As the symmetry breaks, additional excited states with large oscillator strengths appear in the electronic spectrum. Geometry optimization and spectral predictions were also performed in a uniform external electric field in order to simulate nonequilibrium solvation effects due to the finite relaxation time of solvent molecules. Two asymmetric minima with different depths appear on the resulting PES. The lower minimum has charge localized at one of the two molecular terminal groups which is additionally stabilized by the solvent field, while the higher one has charge localized on another terminal group. This finding demonstrates the possibility that two forms with different charge distributions coexist in polar solvents. Our results suggest that nonequilibrium solvation may be a cause of absorption band broadening and splitting. This work is a first step in a larger study aimed at the analysis of the linear and nonlinear properties of long π-conjugated systems of interest for NLO applications and plastic photovoltaics.   © 2009 Wiley Periodicals, Inc. Int J Quantum Chem 109: 3592–3601, 2009

1. Introduction

Linear conjugated organic molecules, exhibiting strong nonlinear optical (NLO) response properties, are of substantial interest for a variety of technological applications, such as laser dyes [1, 2], photosensitizers [3], active molecules in tunable light-emitting diodes [4–6], fluorescent probes in chemistry and biology [7, 8], memory devices [9], etc. Cyanine and cyanine-like dyes, containing heterocyclic terminal groups with their own π-conjugated system, exhibit strong absorption that is easily tunable across the visible and near-infrared region [1, 10] which is important for NLO applications [9]. Charge distribution and instabilities play a crucial role in understanding structure-property relations and in developing organic materials with improved NLO properties.

When the charge carrier is introduced into a highly polarized π-conjugated system it can localize in the form of a charge wave (known as polaron), which induces changes of the molecular geometry leading to further stabilization [11–14]. These changes are sometimes referred to as a solitonic wave of alternating bond lengths, also known as a geometrical or topological soliton. In conjugated chains longer than the dimension of the solitonic wave, the soliton becomes mobile and can result in reduced molecular symmetries and contribute to the broadening of the electronic absorption spectra [13]. Charge instabilities and symmetry breaking effects have been extensively investigated in a variety of systems [15–17]. Traditionally the symmetry lowering in a π-conjugated system is explained in terms of Peierls distortion [18]. A number of theoretical [19–21] and experimental [22] studies have been reported on the symmetry breaking in similar systems. Detailed AM1, DFT, and

$$(H_3C)_2N^+{=}CH{-}(CH{=}CH)_n{-}N(CH_3)_2$$

FIGURE 1. Streptocyanine cations studied in this work.

time-dependent DFT (TD-DFT) calculations were performed by Fabian for polymethine dyes in the gas phase and in polar solvents simulated the polarizable continuum model (PCM) [23]. Semiempirical and ab initio calculations reported by Rabitsky et al. [13] have also indicated that the movement of charge waves in symmetrical cyanine dyes with various terminal groups could lead to symmetry breaking in the electron density distribution and equilibrium molecular geometry. These authors also concluded that unsubstituted $H_2C^+{-}(CH{=}CH)_n{-}CH{=}CH_2$ polymethines retain their symmetry regardless of the chain length (n). Theoretical investigations on the electronic spectra of organic molecules with the long conjugated chains at various theory levels (semiempirical [24–26], time-dependent Hartree–Fock [27], and TD-DFT [27–29, 30]) have also been reported.

Plausible experimental evidence of symmetry breaking in substituted polymethines has been reported [10, 31]. In polar solvents, long chain polymethines display a broad absorption band divided into two sub-bands instead of one single narrow band. The relative ratio between these two sub-bands depends on the solvent polarity. This phenomenon can be explained by the coexistence in the ground state of two molecular forms with the symmetrical and asymmetrical charge distributions [32]. Another possible explanation of the band broadening in the near infrared region is based on the formation of a stable asymmetrical form with two localized charge waves within the conjugated chain.

The goal of this work is to investigate the mechanism of symmetry breaking in a series of cationic streptocyanines with different lengths of conjugation, presented in Figure 1, and to qualitatively predict their absorption properties. We intend to (1) determine the critical number of carbon atoms in the conjugated chain necessary to break the symmetry; (2) construct the ground state potential energy surface (PES) in order to estimate the energy barrier to symmetry breaking in the gas phase and in the solvent; and (3) evaluate the electronic absorption spectra. This is a methodological investigation aimed to establish the protocol suitable to

study more complicated systems of interest for NLO applications.

2. Computational Details

All calculations were carried out using the Gaussian 2003 suite of programs [33]. Because of the size of the molecular systems and limited computational resources, the 6–31G* basis set was used. In a recent benchmark study [34] the restricted Hartree–Fock (RHF) method in combination with basis sets of modest size was shown to reproduce the experimental X-ray geometry of conjugated molecules considerably better than DFT methods, probably because of error cancellation. In addition, excitation energies of both one- and two-photon absorbing states in conjugated molecules were better reproduced at the TD-DFT level with B3LYP exchange-correlation functional when RHF geometries were used [35]. For these reasons the TD-B3LYP/6-31G*//RHF/6-31G* theory level was adopted in this study to predict the transition energies and oscillator strengths for electronic excitations. Molecular geometries were fully optimized both with C_{2v} symmetry and without symmetry constraints. Vibrational frequencies for normal modes were calculated in the harmonic approximation to characterize optimized geometries as either minima or transition states on the PES. The minimum energy path from the symmetric transition state into the asymmetric energy minimum was found using the intrinsic reaction coordinate (IRC) method [36]. The potential energy surface was scanned in two dimensions: along the symmetry adapted (SA) and symmetry breaking (SB) coordinates. The SA coordinate was defined as half the sum of the two central C—C bond lengths in the chain, while the SB coordinate was defined as half the difference of these bond lengths. During the potential energy scan the SA coordinate remained fixed at its optimum value in the corresponding molecular cation with C_{2v} symmetry. The relaxed PES scan was conducted in consecutive steps of constrained geometry optimizations. At each step of the scan one of the central C—C bonds was shortened, while the other one was elongated by the same amount, and all other geometrical parameters were optimized. The same technique was repeated for all the structures in the streptocyanine series (see Fig. 1). The IRC path was reasonably reproduced by relaxed PES scan of the symmetry breaking reaction coordinate. Calculations were
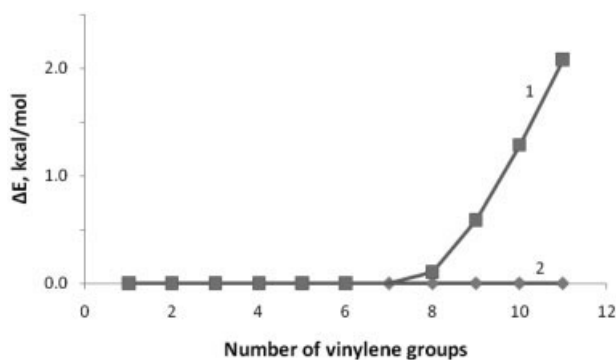
FIGURE 2. Symmetry breaking in streptocyanine cations. ΔE is the energy difference between asymmetric (squares, Curve 1) and symmetric (diamonds, Curve 2) structures for different numbers of vinylene groups. [Color figure can be viewed in the online issue, which is available at www.interscience.wiley.com.]

performed for both gas and solution phases. We employed both the polarizable continuum model (PCM) and uniform external electric field to examine the equilibrium and nonequilibrium [37] (related to the finite relaxation time of the solvent molecules) solvent effects on the PES and electronic spectra [38]. The keywords used were SCRF = (PCM, Solvent = Heptane) and Field = X − 1, respectively.

3. Results and Discussion

The symmetric structures of the shorter molecules in the series proved to be true minima on the PES, as confirmed by all positive eigenvalues of the Hessian matrix during the frequency calculations. For longer chains, the symmetric structure proved to be a transition state; the normal mode associated with the imaginary frequency showed single-double bond length alternations within the polymethine chain. The critical number n of vinylene (—CH=CH—) groups where the symmetry lowering occurs, was determined. These results are shown in Figure 2. They suggest that, at the RHF/6-31G* theory level, streptocyanine cations break symmetry at eight vinylene groups, in agreement with the previous study [13]. The difference in energy between the higher (C_{2v}) and lower symmetry (C_s) structures can be used to measure the symmetry breaking effect. Figure 2 can also be used to identify the shortest symmetry broken chain length for the longer conjugated structures and avoid the

computationally expensive calculations of second derivatives. According to the previous study of polymethine dyes, the RHF method underestimates the chain length at which symmetry lowering occurs, while at the B3LYP level the symmetry breaking was not observed [23]. In agreement with these findings, we did not observe symmetry lowering at the B3LYP/6-31G* theory level up to 15 vinylene groups. It is known that a pure DFT method overestimates charge delocalization due to the self-interaction error [39], with electron-electron repulsion predicted even in one-electron systems. This error is reduced but not completely eliminated in the hybrid DFT approaches. On the other hand, wavefunction theory methods that include electron correlation may also overestimate charge delocalization [40]. Thus, different theoretical methods (B3LYP, RHF) predict charge localization at different chain lengths. The choice of a particular method extends beyond the scope of the present work. Instead, we focus here on the protocol of plotting PES, evaluating the energy barrier generated by symmetry breaking, and predicting electronic spectra for the symmetrical and the symmetry-broken structures.

Next we used a relaxed scan along the SB-coordinate to plot the profile of the ground state potential energy surface and examine the possibilities for multiple minima, including symmetrical and asymmetrical forms. This scan for the shortest symmetry broken structure ($n = 8$) is presented in Figure 3. The relatively low energy barrier suggests that the
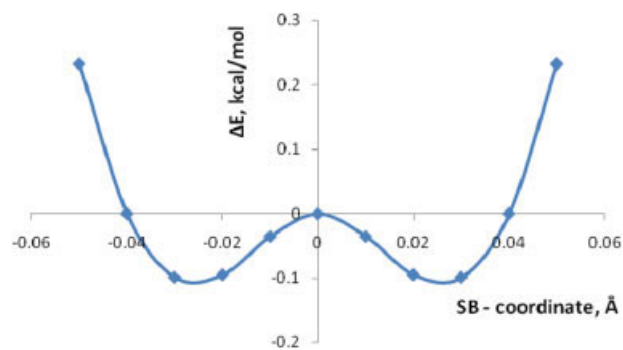

FIGURE 3. One-dimensional potential energy scan along the symmetry breaking reaction coordinate (SB) for streptocyanine with eight vinylene groups ($n = 8$). ΔE is the energy difference between the energies of the transition state and the corresponding structures along the SB-coordinate. [Color figure can be viewed in the online issue, which is available at www.interscience.wiley.com.]
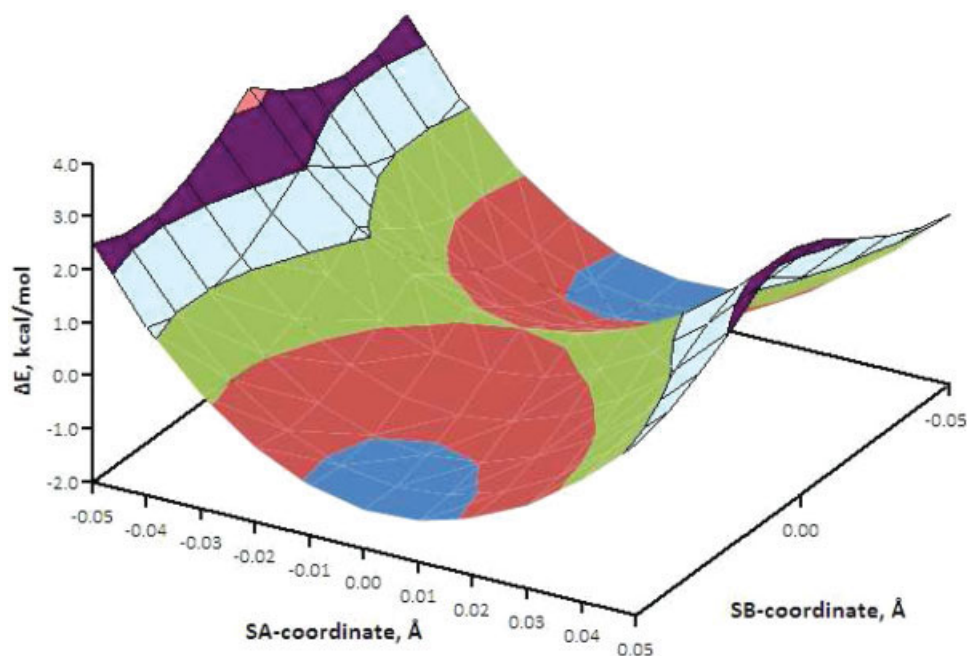
FIGURE 4. Two-dimensional potential energy surface cross-section for streptocyanine with 10 vinylene groups ($n =$ 10) along the symmetry adapted (SA) and the symmetry breaking (SB) coordinate. Each color corresponds to another 1 kcal/mol step. [Color figure can be viewed in the online issue, which is available at www.interscience.wiley.com.]

symmetry lowering may occur at longer chain lengths after zero point vibrational energy is taken into account. As the chain length increases, the magnitude of the barrier increases significantly. To examine the possibilities for coexistence of both symmetrical and symmetry broken forms, we performed a two-dimensional scan (along SB and SA coordinates) for the streptocyanine with 10 vinylene groups as shown in Figure 4. This technique can be used to evaluate the multidimensional PES for the ground and excited states of π-conjugated systems. One can see from the resulting plot that motion along the SB coordinate connects the two C_s symmetric minima on the surface and passes over an energy barrier. The top of this barrier between the two minima corresponds to a transition state geometry of C_{2v} symmetry. These minima correspond to the symmetry broken geometries which belong to C_s point group symmetry. As the chain length is increased the barrier height increases, which corresponds to a relative stabilization of the asymmetrical form. It follows from our data that we have not found the multiple minima corresponding to simultaneous existence of the symmetrical and asymmetrical forms in the gas phase.

We also used the relaxed scan technique described earlier to evaluate the PES for different chain lengths in the nonpolar solvent cyclohexane. We employed the PCM methodology to account for equilibrium solvent effects in our calculations. The results are shown in Figure 5. As in the gas phase, we have observed a symmetrical double well po-
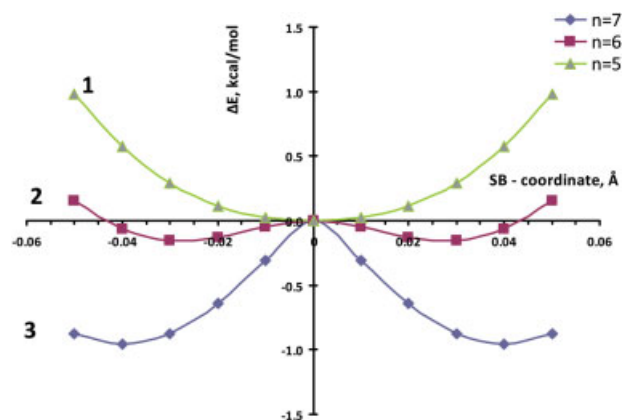

FIGURE 5. One-dimensional relaxed potential energy scan along the symmetry breaking coordinate (SB) for streptocyanine cations with $n = 5$ (Curve 1), 6 (Curve 2), and 7 (Curve 3) in cyclohexane. The energies plotted relative to the energy of the C_{2v} symmetric structure. [Color figure can be viewed in the online issue, which is available at www.interscience.wiley.com.]

tential for the symmetry broken structures and a single minimum for the symmetrical structures. As expected, symmetry lowering in solution was observed at a shorter chain length of $n = 6$ as compared to $n = 8$ in the gas phase. A similar effect of symmetry breaking was found in quantum mechanical studies of nitrate ion with explicit solvent [41].

The PCM model implicitly accounts for both electronic and orientational polarization of the solvent. The dielectric response of the solvent is assumed to be much faster than intramolecular geometry and charge relaxation. However, bond length alternation and especially charge localization in streptocyanines are ultra fast processes that may be several orders of magnitude faster than reordering of the polar solvent molecules around the solute. If the charge wave movement within the conjugated chain occurs faster than the corresponding solvent rearrangement, then the solvent reaction field, and therefore the potential energy surface, will not be symmetrical at the instant when the charge wave moves. The finite reorientation time of the solvent molecules gives rise to nonequilibrium (or retarded) solvation effects. Related nonequilibrium solvation model is often used to describe the processes of charge transfer [37]. We used an external uniform electric field directed along the molecular chain, instead of the PCM method, to describe the nonequilibrium effects of the polar solvents. A field of magnitude 10^{-4} a.u. was applied to the streptocyanine with $n = 8$ (first symmetry broken structure for the gas phase) and for two longer dyes with $n = 9$ and 10. The results are shown in Figure 6. As one can see, all the curves appear to have asymmetrical shapes. However, the PES for the structure with $n = 8$ shows a single minimum only, while the structures with $n = 9$ and, especially, $n = 10$ demonstrate double well potential surfaces. Each minimum of the asymmetric double well PESs corresponds to a molecular geometry with charge localized at one of the two molecular terminal groups. Such a geometry might be additionally stabilized by the solvent reaction field and by a reordering of solvent molecules around the solute, and correspond to the lower minimum. The molecular geometry with charge localized at the other molecular terminal groups corresponds to a higher minimum on PESs. This demonstrates that for long conjugated chromophores in polar solution there is a possibility of coexistence of the two forms with different charge localization within the chain surrounded by adjusted solvent shells. Our results
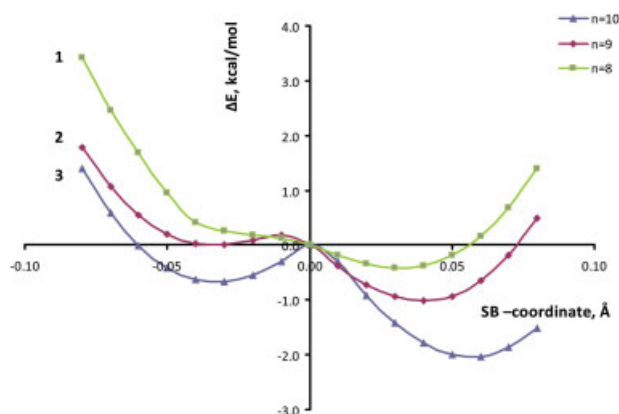

FIGURE 6. One-dimensional PES scan along the symmetry breaking reaction coordinate (SB) in streptocyanines with $n = 8$ (Curve 1), $n = 9$ (Curve 2), and $n = 10$ (Curve 3) in the presence of an electric dipole field aligned along the conjugated chain. [Color figure can be viewed in the online issue, which is available at www.interscience.wiley.com.]

suggest that this methodology can be used successfully for the qualitative description of equilibrium and nonequilibrium solvent effects.

The Mulliken charges on the atoms of the conjugated chain of length $n = 10$ are plotted in Figure 7, including the nitrogen atoms of the terminal groups. The first three plots correspond to the charge distribution for the PES minimum at the negative SB coordinate (see Fig. 6) calculated in the gas phase [Fig. 7(a)], in cyclohexane [Fig. 7(b)], and in an external electric field [Fig. 7(c)]. Figure 7(d) illustrates the charge distribution for the PES lower minimum at the positive SB coordinate (see Fig. 6). One can see that charges on the even and odd atoms tend to alternate. A similar charge alternation was observed in polyenes [42], and connected to bond length alternation. Geometrical symmetry breaking causes the charge to localize at one of the terminal groups, thereby leading to an asymmetric charge distribution at the equilibrium geometries. Moreover, charge localization becomes more pronounced as the depth of the potential increases. This effect is manifested in Figure 7(b) and it is even more distinct in Figure 7(d).

We also calculated the vertical absorption spectra at the TD-B3LYP/6-31G* level of theory at RHF/6-31G* optimized geometry for members of the streptocyanine series with $n = 1–10$ in the gas phase, $n = 5–7$ in cyclohexane, and for the two geometries when $n = 9$ in the external electric field. They are shown on Figure 8. As can be seen for the
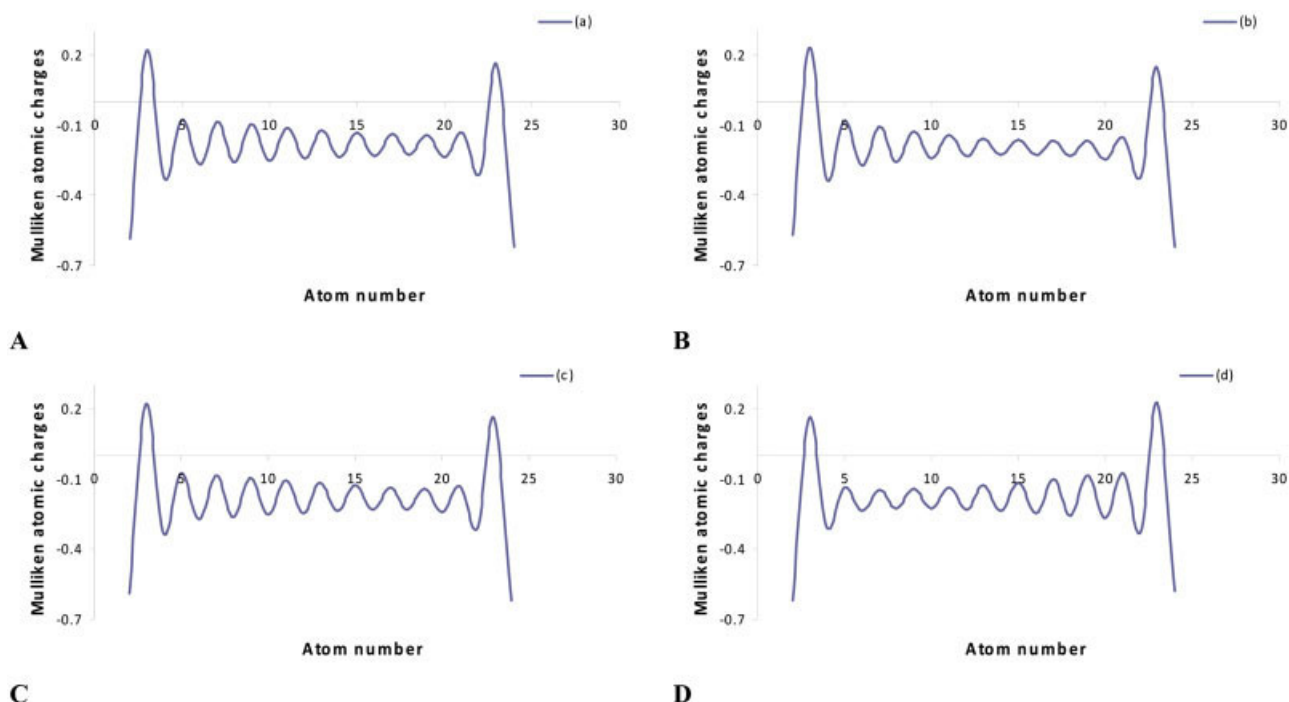
FIGURE 7. Mulliken atomic charges along the conjugated chain for streptocyanine cation with $n = 10$. The plots correspond to the structures at the energy minima calculated in: (a) gas phase, (b) cyclohexane, (c) higher, and (d) lower minimum in an external electric field. [Color figure can be viewed in the online issue, which is available at www.interscience.wiley.com.]

structures with a conjugated chain length up to $n = 7$ in the gas phase and for $n = 5$ in cyclohexane, TD-DFT predicts only one absorption band. In agreement with the experimental data, lengthening of the conjugated chain leads to a long wavelength shift of the absorption peak. Our calculations show that the oscillator strength for this transition grows linearly with the chain length up to the symmetry breaking point, where the second sub-band appears (at $n = 8$ in the gas phase and $n = 6$ in cyclohexane). The second sub-band grows in oscillator strength with increasing chain length as the lower energy band decreases. For the longer conjugated structures a third peak appears in the absorption spectra. Panel $n = 9$ represents an absorption spectrum for two geometries corresponding to the lower and higher minima of the PES under the external electric field. As seen, application of the field leads to an enhanced absorbance of the second sub-band for the lower minimum geometry and to a suppressed absorbance for the higher minimum as compared to the gas phase. Thus, the spectral broadening in the cyanine compounds can be explained by both in-

tramolecular factors (multiple absorbing states), and by the dynamics of the charge wave in the nonequilibrium solvent reaction field. However, more experimental and theoretical studies are needed to more deeply understand the nature of the absorption bands in long conjugated systems.

4. Conclusions

We investigated the mechanism of symmetry breaking in a series of cationic streptocyanines with different conjugated chain lengths and qualitatively predicted their electronic absorption spectra. This class of organic molecules is chosen as a model system to develop the methodology which can subsequently be used to evaluate more complicated compounds for NLO applications. Our calculations show that the minimum number of vinylene groups in the conjugated chain necessary to break the symmetry of streptocyanines is eight in the gas phase and six in cyclohexane.

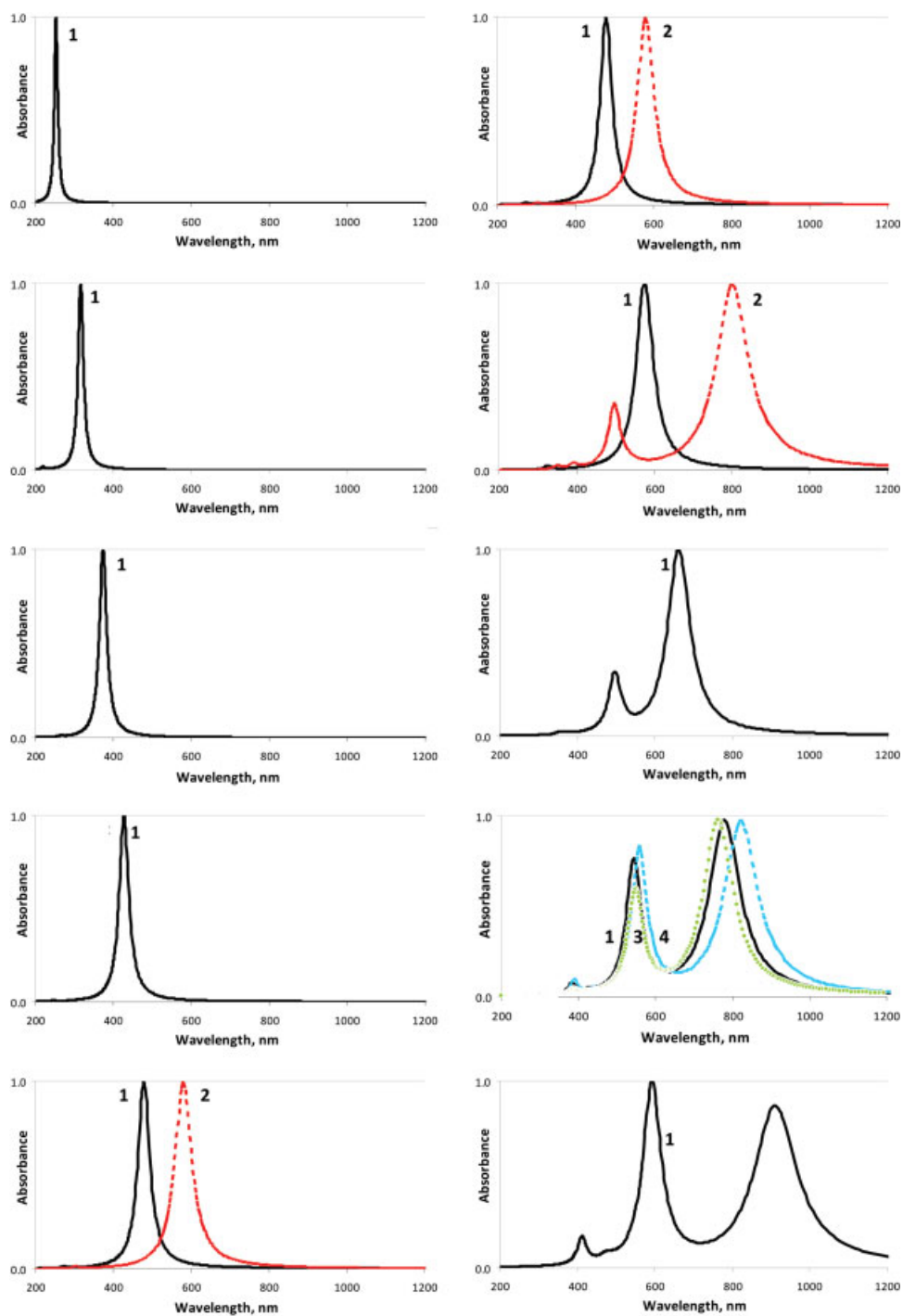We constructed the ground state potential energy surface in two dimensions, using symmetry

FIGURE 8. Electronic absorption spectra calculated at the TD-B3LYP/6-31G*//RHF/6-31G* level for streptocyanine cation with n = 1–10 in the gas phase (Curve 1, black), cyclohexane (Curve 2, red), and in the electric field for molecular geometries at the higher minimum (Curve 3, green) and the lower minimum (Curve 4, turquoise). [Color figure can be viewed in the online issue, which is available at www.interscience.wiley.com.]

breaking (SB) and symmetry adapted (SA) coordinates, defined as difference and sum of the two central C—C bonds. This PES was found to have

two equivalent minima corresponding to symmetry broken geometries that belong to the point group C_s. The energy peak between these two minima

corresponds to the transition state with the point group C_{2v}. Its value was estimated for systems with the different chain lengths in the gas and solution phases, the latter being modeled by the polarizable continuum model. As the symmetry breaks, additional absorption bands with large oscillator strength appear in the electronic spectrum.

Charge localization is additionally stabilized by the solvent reaction field, which increases the energy barrier and results in symmetry broken geometries at a shorter (than in the gas phase) length of the conjugated system. The electronic absorption spectrum in solution is red shifted as compared to the gas phase in agreement with the experimental results.

Geometry optimization and spectral predictions were also obtained using a uniform external electric field to simulate nonequilibrium (or retarded) solvation effects involving slow solvent reorientation processes in polar media. Two asymmetric minima with different depths appear on the resulting potential energy surface. The lower minimum corresponds to a molecular geometry with charge localized at one of the two molecular terminal groups which is additionally stabilized by the solvent field. The higher minimum corresponds to charge localization at another terminal group. This finding demonstrates the possibility of coexistence of the two forms in polar solution. Thus our results suggest that nonequilibrium solvation may be an important factor in absorption band broadening.

This work is a first step in the broader study aimed at the analysis of the linear and nonlinear properties of long π-conjugated systems of interest for organic NLO applications and plastic photovoltaics.

References

1. Fabian, J.; Nakazumi, H.; Matsuoka, M. Chem Rev 1992, 92, 1197.
2. Kaschke, M.; Ernsting, N. P.; Valeur, B.; Bourson, J. J Phys Chem 1990, 94, 5757.
3. Naber, A.; Fischer, U. C.; Kirchner, S.; Dziomba, T.; Kollar, G.; Chi, L. F.; Fuchs, H. J Phys Chem B 1999, 103, 2709.
4. Baldo, M. A.; O'Brien, D. F.; You, Y.; Shoustikov, A.; Sibley, S.; Thompson, M. E.; Forrest, S. R. Nature 1998, 395, 151.
5. Bulovic, V.; Shoustikov, A.; Baldo, M. A.; Bose, E.; Kozlov, V. G.; Thompson, M. E.; Forrest, S. R. Chem Phys Lett 1998, 287, 455.
6. Bulovic, V.; Deshpande, R.; Thompson, M. E.; Forrest, S. R. Chem Phys Lett 1999, 308, 317.
7. Seifert, J. L.; Connor, R. E.; Kushon, S. A.; Wang, M.; Armitage, B. A. J Am Chem Soc 1999, 121, 2987.
8. Hung, S. C.; Ju, J. Y.; Mathies, R. A.; Glazer, A. N. Anal Biochem 1996, 243, 15.
9. Emmelius, M.; Pawlowski, G.; Vollmann, H. W. Angew Chem Int Ed Engl 1989, 28, 1445.
10. Tolbert, L. M.; Zhao, X. D. J Am Chem Soc 1997, 119, 3253.
11. Craw, J. S.; Reimers, J. R.; Bacskay, G. B.; Wong, A. T.; Hush, N. S. Chem Phys 1992, 167, 101.
12. Reimers, J. R.; Hush, N. S. Chem Phys 1993, 176, 407.
13. Ryabitsky, A. B.; Kachkovski, A. D.; Przhonska, O. V. J Mol Struct (THEOCHEM) 2007, 802, 75.
14. Heeger, A. J.; Kivelson, S.; Schrieffer, J. R.; Su, W. P. Rev Mod Phys 1988, 60, 781.
15. Gammel, J. T.; Saxena, A.; Batistic, I.; Bishop, A. R.; Phillpot, S. R. Phys Rev B 1992, 45, 6408.
16. Anusooya-Pati, Y.; Soos, Z. G.; Painelli, A. Phys Rev B 2001, 6320, 10.
17. Prassides, K.; Schatz, P. N.; Wong, K. Y.; Day, P. J Phys Chem 1986, 90, 5588.
18. Peierls, R., Ed. Quantum Theory of Solids; Oxford University Press: New York, 1955.
19. Tyutyulkov, N.; Drebov, N.; Dietz, F. Chem Phys 2005, 310, 297.
20. Zuppiroli, L.; Bieber, A.; Michoud, D.; Galli, G.; Gygi, F.; Bussac, M. N.; Andre, J. J. Chem Phys Lett 2003, 374, 7.
21. Geskin, V. M.; Cornil, J.; Bredas, J. L. Chem Phys Lett 2005, 403, 228.
22. Terenziani, F.; Painelli, A.; Katan, C.; Charlot, M.; Blanchard-Desce, M. J Am Chem Soc 2006, 128, 15742.
23. Fabian, J. J Mol Struct (THEOCHEM) 2006, 766, 49.
24. Grozema, F. C.; Candeias, L. P.; Swart, M.; van Duijnen, P. T.; Wildeman, J.; Hadziioanou, G.; Siebbeles, L. D. A.; Warman, J. M. J Chem Phys 2002, 117, 11366.
25. Cornil, J.; Beljonne, D.; Bredas, J. L. J Chem Phys 1995, 103, 834.
26. Cornil, J.; Beljonne, D.; Bredas, J. L. J Chem Phys 1995, 103, 842.
27. Hirata, S.; Head-Gordon, M.; Bartlett, R. J. J Chem Phys 1999, 111, 10774.

28. Stratmann, R. E.; Scuseria, G. E.; Frisch, M. J. J Chem Phys 1998, 109, 8218.

29. Hirata, S.; Head-Gordon, M. Chem Phys Lett 1999, 314, 291.

30. Salzner, U. J Phys Chem A 2008, 112, 5458.

31. Brooker, L. G. S.; Craig, A. C.; Heseltin, Dw.; Jenkins, P. W.; Lincoln, L. L. J Am Chem Soc 1965, 87, 2443.

32. Lepkowicz, R. S.; Przhonska, O. V.; Hales, J. M.; Fu, J.; Hagan, D. J.; Van Stryland, E. W.; Bondar, M. V.; Slominsky, Y. L.; Kachkovski, A. D. Chem Phys 2004, 305, 259.

33. Frisch, M. J.; Trucks, G. W.; Schlegel, H. B.; Scuseria, G. E.; Robb, M. A.; Cheeseman, J. R.; Montgomery, J. A., Jr.; Vreven, T.; Kudin, K. N.; Burant, J. C.; Millam, J. M.; Iyengar, S. S.; Tomasi, J.; Barone, V.; Mennucci, B.; Cossi, M.; Scalmani, G.; Rega, N.; Petersson, G. A.; Nakatsuji, H.; Hada, M.; Ehara, M.; Toyota, K.; Fukuda, R.; Hasegawa, J.; Ishida, M.; Nakajima, T.; Honda, Y.; Kitao, O.; Nakai, H.; Klene, M.; Li, X.; Knox, J. E.; Hratchian, H. P.; Cross, J. B.; Adamo, C.; Jaramillo, J.; Gomperts, R.; Stratmann, R. E.; Yazyev, O.; Austin, A. J.; Cammi, R.; Pomelli, C.; Ochterski, J. W.; Ayala, P. Y.; Morokuma, K.; Voth, G. A.; Salvador, P.; Dannenberg, J. J.; Zakrzewski, V. G.; Dapprich, S.; Daniels, A. D.; Strain, M. C.; Farkas, O.; Malick, D. K.; Rabuck, A. D.; Raghava-chari, K.; Foresman, J. B.; Ortiz, J. V.; Cui, Q.; Baboul, A. G.; Clifford, S.; Cioslowski, J.; Stefanov, B. B.; Liu, G.; Liashenko, A.; Piskorz, P.; Komaromi, I.; Martin, R. L.; Fox, D. J.; Keith, T.; Al-Laham, M. A.; Peng, C. Y.; Nanayakkara, A.; Challacombe, M.; Gill, P. M. W.; Johnson, B.; Chen, W.; Wong, M. W.; Gonzalez, C.; Pople, J. A. Gaussian, Inc., Wallingford, 2004.

34. Belfield, K. D.; Bondar, M. V.; Hernandez, F. E.; Masunov, A. E.; Mikhailov, I. A.; Morales, A. R.; Przhonska, O. V.; Yao, S. J Phys Chem C 2009, 113, 4706.

35. Masunov, A. M.; Tretiak, S. J Phys Chem B 2004, 108, 899.

36. Fukui, K. Acc Chem Res 1981, 14, 363.

37. Basilevsky, M. V.; Chudinov, G. E. Chem Phys 1991, 157, 327.

38. Miertus, S.; Scrocco, E.; Tomasi, J. Chem Phys 1981, 55, 117.

39. Cohen, A. J.; Mori-Sanchez, P.; Yang, W. T. Science 2008, 321, 792.

40. Wannere, C. S.; Sattelmeyer, K. W.; Schaefer, H. F.; Schleyer, P. V. Angew Chem Int Ed 2004, 43, 4200.

41. Lebrero, M. C. G.; Bikiel, D. E.; Elola, M. D.; Estrin, D. A.; Roitberg, A. E. J Chem Phys 2002, 117, 2718.

42. Canuto, S.; Calais, J. L.; Goscinski, O. J Phys B Atom Mol Opt Phys 1981, 14, 1409.